arXiv:1501.04472v1 [cond-mat.soft] 19 Jan 2015

Local analysis of the history dependence in tetrahedra packings

N. Nirmal Thyagu, Max Neudecker, and Matthias Schröter

January 20, 2015

The mechanical properties of a granular sample can depend on the way the packing was prepared. However, the variables which store this information are often unknown. Here we present an X-ray tomography study of tetrahedra packings prepared with three different tapping strengths. Our main result is that the relative contribution of the three different contact types possible between tetrahedra – face-to-face (F2F), edge-to-face (E2F), and point contacts – is one variable which stores the preparation history. We show this by preparing pairs of packings that differ either in their bulk volume fraction ϕ_{global} or in their number of mechanical constraints per particle C, where C is determined from all three contact types which each fix a different amount of constraints. For the pairs with the same ϕ_{global} the number of E2F and point contacts varies with preparation, while the number of F2F contacts stays constant. For the iso-constraint packings the relative contribution of all three contact types stays the same. We then perform a local analysis of the contact distribution by grouping the particles together according to their individual volume fraction ϕ_{local} computed from a Voronoi tessellation. We find that the probability distribution of ϕ_{local} depends only on ϕ_{global}, not on C. The number of F2F and E2F contacts increases in all experiments with ϕ_{local}; the number of point contacts, while always being the largest, decreases with ϕ_{local}. However, only the number of F2F contacts can be described by an universal function of ϕ_{local}. This behavior differs from spheres and ellipsoids and posses a significant constraint for any mean-field approach to tetrahedra packings.

1 History dependence in granular matter

The mechanical properties of a granular sample are known to depend on the way the sample was prepared. Examples include the volume response to shear[1], the increase of pressure with depth in a granular column[2–5], or the density distribution inside[6] respectively the pressure distribution[7] below a sandpile. Another type of history dependent behavior which is sometimes referred to as memory effect can be seen if a sample is compactified, e.g. by shearing or tapping with a driving strength s_i, to a specific volume fraction ϕ_{global}. If then the driving strength is changed to s_0 it is found that the subsequent evolution of ϕ_{global} differs for different values of s_i[8,9]. A similar effect can be found in granular gases[10].

In some sense the term history dependence simply expresses the fact that ϕ alone does not provide a complete description of state of the packing. Given that the mechanical properties of the sample originate from forces transmitted between particles at contacts it seems natural to extend the description by including information on a) the number and spatial structure of the contacts and b) the distribution of contact forces. The second option is directly connected to the fact that frictional packings at finite pressures are hyperstatic[11–14] i.e. there exist many possible force configurations which fulfill a given boundary conditions[15]. The distribution of contact forces has presently only be measured in two-dimensional systems of compressive[16] or photoelastic[17] discs, the latter experiment finds a clear dependence on the preparation protocol. In principle the preparation history could also be stored in distribution of the Voronoi volumes surrounding each particle, but at least for spheres neither the volume distribution[18] nor the shape distribution[19] showed any signature of the preparation conditions. In this work we will study tetrahedra packings both with respect to the number and type of contacts and the properties of their Voronoi volumes.

Several theoretical approaches to sphere packings are based on the average number of contacts Z of each particle. For example the jamming paradigm[20,21] assumes that mechanical properties depend only on the difference ΔZ between the actual contact number and the minimum number required to constrain all particles (the so called isostatic condition). ΔZ is then assumed to depend on ϕ_{global} only. However, for frictional particles the formation of contacts is controlled by parameters defined on the grain level[22]. This is for example taken into account by a statistical mechanics approach to static granular media[23] where Z is computed from a mean-field approximation of ϕ_{local}. Similarly, the granocentric model[24–26] predicts the probability distribution of Z in jammed emulsions and disk packings using grain level arguments.

But even the notion that ϕ_{global} and Z amount to a complete description of sphere packings has been challenged. The value of Z at the Random Close Packing (RCP) density depends e.g. on the numerical protocol used to prepare the sphere

---

[0] *Max Planck Institute for Dynamics and Self-Organization (MPIDS), 37077 Goettingen, Germany*

[0] *n*irmal.thyagu@ds.mpg.de

[0] *m*atthias.schroeter@ds.mpg.de

packing[27]. And for frictional disks it has been shown that in the ϕ_{global} range between RCP and dilatancy onset[28] mechanical stability requires a fabric tensor anisotropy larger than a certain threshold[29].

2 Packings of tetrahedra

History dependence is not limited to sphere packings, recently we demonstrated that packings of tetrahedra with the same ϕ_{global} can differ in their values of C and Z depending on how the sample was prepared[30]. Such tetrahedra packings have recently been an active field of research with experimental studies of their mechanical properties under uniaxial compression[31,32] and their limits of mechanical stability[33]. The jamming of frictionless tetrahedra has been addressed by both simulations[34–41] and a mean field approach[42,43].

Contrary to spheres, tetrahedra have 4 different types of contacts: face-to-face (F2F) contacts, which are mechanically equivalent to 3 individual point contacts, edge-to-face (E2F) contacts (equivalent to two point contacts) and the vertex-to-face (V2F) and edge-to-edge (E2E) contacts which we group her as point contact. This distinction is important because the different contact types fix each a different number of degrees of freedom. The total number of constraints C equals therefore $\sum_i C_i Z_i$ where i goes over the three contact types (F2F, E2F, point), Z_i is the respective contact number and C_i are the number of constraints per particle fixed at this type of contact. The different values of C_i can be understood for frictional contacts as follows: All contacts impose 3 translational constraints, E2F contacts add 2 rotational constraints, F2F contacts prohibit 3 different rotations. As these constraints are shared between two tetrahedra, we obtain the constraint multipliers $C_{F2F} = 3.0$, $C_{E2F} = 2.5$, and $C_{V2F} = C_{E2E} = 1.5$.

Each tetrahedron has 6 degrees of freedom (3 translations and 3 rotations), therefore a mechanical stable packing requires at least $C = 6$, the so called isostatic case. However, typical experimental packings of frictional tetrahedra have C values in the range 12 to 18 and are therefore strongly hyperstatic[30]. Contrary claims of isostaticity[44] are based on the use of frictionless constraint multipliers when analyzing experimental i.e. frictional packings. Because of the importance of the constraint number for the mechanical properties, we will discuss in the remainder of this paper C rather than Z.

3 Experimental setup

Experiments were performed with the same polypropylene tetrahedra as in reference[30]. The particles, figure 1 a) shows an example, were made by mould casting, their edge length is 7 mm and their coefficient of static friction equals 0.8[45].

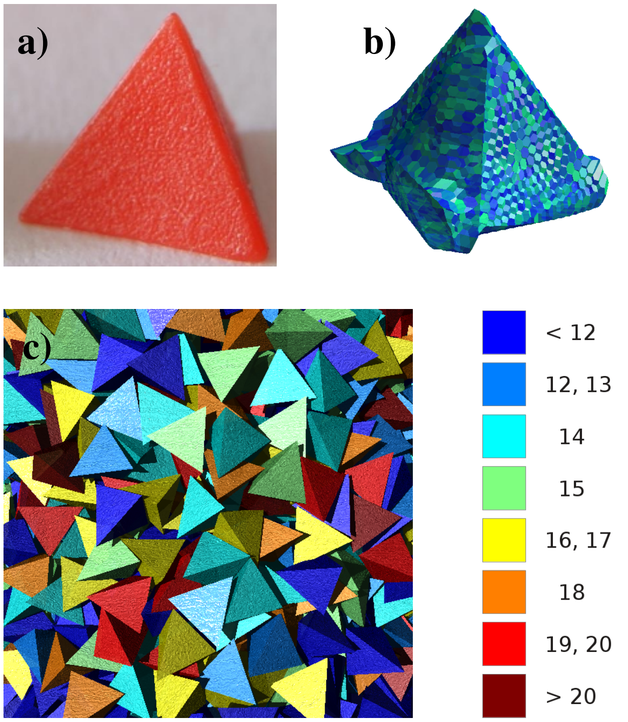

Figure 1 Tetrahedra packing. **a)** Polypropylene particle made by injection moulding, the edge length is 7mm. **b)** Voronoi Cell around a particle. **c)** Rendering of an interior section of a tetrahedra packing after all particles have been identified from an X-ray tomogram. Particles are colored according to the number of constraints fixed by their neighbors. The global volume fraction is 0.54, the average constraint number is 14.1.

Packings were prepared by tapping, starting from a loose initial configuration which was prepared by first filling the particles into a smaller inner cylinder (without bottom) and then releasing them into a larger cylindrical container of diameter 10.4 cm by slowly moving the inner cylinder upwards. Tapping is done with an electromagnetic shaker (LDS model V555) which is driven by a series of sinusoidal pulses with a frequency f = 3 Hz. The separation between individual pulses is 0.5 s, the amplitude of the sinusoidal motion is chosen such that the peak acceleration Γ corresponds to either 2g, 5 g, or 7g where g is the acceleration due to gravity.

To monitor the evolution of ϕ_{global} during tapping, height profiles of the packing are measured in regular intervals with a laser distance sensor (MicroEpsilon ILD1402) mounted on a horizontal translation stage. These readings are then corrected for boundary effects by calibrating them with the bulk ϕ_{global} values measured from the tomographic reconstructions. After the packings have been prepared, three-dimensional images of the geometrical arrangement of particles are obtained by X-ray tomography (Nanotom, GE) with a resolution of 100 μm per

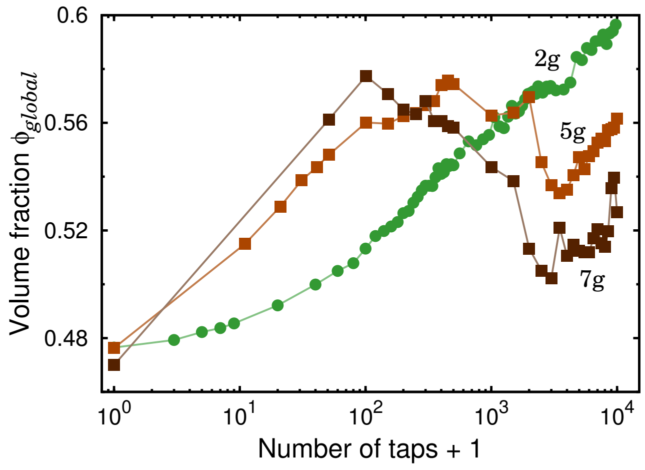

Figure 2 Compaction of tetrahedra packings for three different tapping strengths $\Gamma = 2g, 5g$ and $7g$.

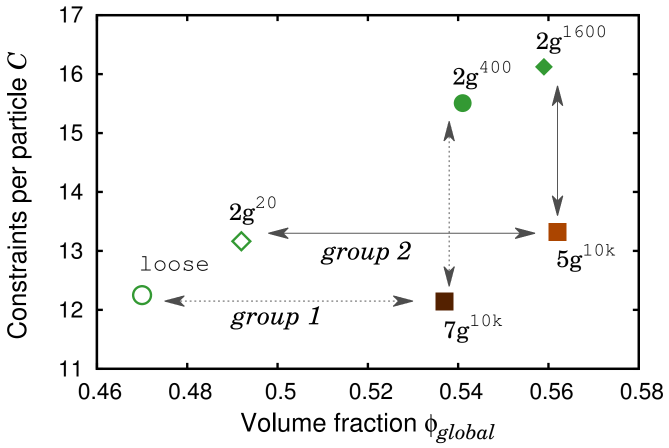

Figure 3 History dependent preparation. By choosing the number and strength of taps during preparation, we can prepare iso-constraint pairs of experiments with different ϕ_{global} at similar C (indicated by horizontal arrows) and iso-volume fraction pairs which differ only in C not in ϕ_{global} (vertical arrows).

voxel.

3.1 Image analysis

Particles are identified by a two step algorithm involving a cross-correlation with an inscribed sphere and a steepest ascend gradient search; the particle detection rates are better than 99.8 %. After the positions and orientations of all particles are known, the number and type of contacts is computed for each particle. Figure 1 c) displays a rendering of a cross section through the bulk of a sample where the individual tetrahedra are color coded according to their number of constraints. Further details on these processing steps can be found in the supplementary information of[30]. Similar to reference[30] all particle positions are available for download from Dryad[46].

3.2 Preparing packings

Figure 2 demonstrates the evolution ϕ_{global} with the number of taps. For a tapping strength Γ = 2g there is a monotonic increase in ϕ_{global}. In contrast, at Γ = 5g and 7g the volume fraction first grows and then decreases and finally grows again. In none of the experiments a steady state is reached; in reference[30]it is shown that at least 10^5 taps are needed at Γ = 2g for reaching a plateau in ϕ_{global}.

As already shown in reference[30] the number of constraints in a tetrahedra packing does not only depend on ϕ_{global} but also on the tapping protocol used to prepare the sample. This allows us to prepare two pairs of *iso-volume fraction* samples i.e. they have same the value of ϕ_{global} but which differ in C. Figure 3 shows these two pairs, one of them is labeled $7g^{10k}$ and $2g^{400}$, the other is $5g^{10k}$ and $2g^{1600}$. The main number number indicates the Γ value used during preparation, the superscripts denotes the number of taps.

Our second comparison is between two pairs of packings that have approximately the same value of C, but different volume fraction ϕ_{global}. We will refer to them as *iso-constraint* pairs. They are also displayed in figure 3 using the labels $7g^{10k}$ and loose (i.e. packing has not been tapped at all); the second pair is $5g^{10k}$ and $2g^{20}$.

4 Comparing global values of iso-constraint and iso-volume fraction packings

The tables in the top right panels of figures 4 and 5 list the ϕ_{global} and C values of all six experiments discussed in this paper. The tables also show the contribution of the three different contact types towards the total number of constraints. In all experiments the overwhelming majority of constraints is contributed by the point and E2F contacts.

For an evaluation of the relative changes within the pairs an estimate for the experimental error is required. As shown in the supplements of reference[30] the detection of the total number of contacts has an approximate statistical error of $\pm$ 0.2. Unfortunately, we can not derive an error estimate for the algorithm assigning the different contact types. We will therefore consider $\pm$ 0.2 C_i as a best case approximation of our actual errors; this corresponds to $\pm$ 0.3 for C_{point}, $\pm$ 0.5 for C_{E2F}, and $\pm$ 0.6 for C_{F2F}.

Within these error estimates the relative contribution of the three contact types seems to stay constant for the *iso-constraint* pairs, at least in a first approximation. (Comparing $5g^{10k}$ and $2g^{20}$ there might be a small conversion of point to F2F contacts.) For the *iso-volume fraction* pairs the increase in C is only due to an increase in the number of point and E2F contacts, not the F2F.

The main conclusion of this global analysis is that theoretical approaches, such as the jamming paradigm, which assume that C is determined by ϕ_{global} alone will not be sufficient to describe packings of frictional tetrahedra.

We will therefore turn to the local-contact paradigm which assumes that the number of contacts a given particle forms will only depend on locally defined variables. These can be either material parameters, such as the fiction coefficient or the aspect ratio α of an ellipsoid. Or parameters which describe the neighborhood of the particle, such as volume or shape of its Voronoi cell. Here the former is often expressed as the local volume fraction ϕ_{local} which is the particle volume divided by the volume of the Voronoi cell. It has recently been shown experimentally that in packings of spheres[47] and ellipsoids[22] the most likely contact number of a particles does only depend on ϕ_{local} (and α in the case of ellipsoids), *not* on ϕ_{global}. Examples of theories compatible with the local-contact paradigm are e.g. the statistical mechanics approach to static granular media[23,42] or the the granocentric model[24,25].

5 Distribution of local volume fractions

For both spheres and ellipsoids the probability distribution of the Voronoi volumes can be rescaled by $(\phi_{local} - \phi_{global})/\sigma(\phi_{global})$ with $\sigma(\phi_{global})$ being the standard deviation of the distribution. The resulting master curve are independent of α[22].

To test the similarity between sphere and tetrahedra packings we have computed the Voronoi volume distribution all six experiments; it is displayed in the lower row of panels in figures 4 and 5.

6 Contact probabilities depend on local volume fraction

The middle row of panels in figures 4 and 5 displays how the contribution of the three different contact types changes with ϕ_{local}. As expected, for all experiments and values of ϕ_{local} the number of constraints fixed by point contacts is the largest contribution. Interestingly however, the slope $dC_{point}/d\phi_{local}$ is negative while it is positive for the E2F and F2F contacts, as it is for contacts between spheres or ellipsoids. This agrees with the intuitive notion that the closer two tetrahedra get to each other, the more likely it is that their flat faces or straight edges aligned with each other and the corresponding contact changes from a point contact to a higher constrained one.

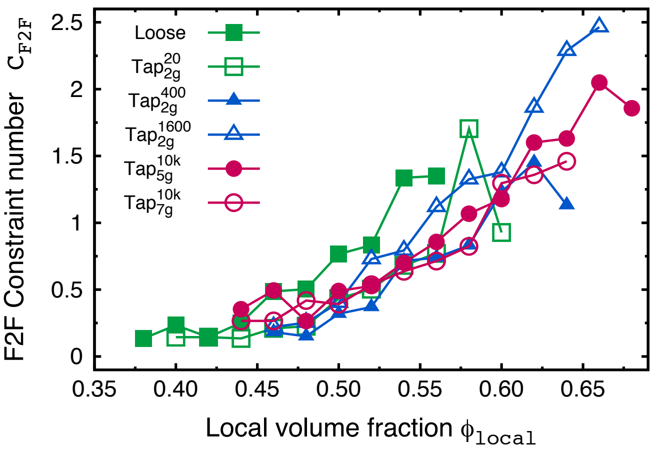

Figure 6 Constraints due to F2F contacts in all six experiments. Included are all bins in ϕ_{local} which amount to at least 1.7 % of the total number of particles.

At the local level the signature of preparation dependence is again clearly visible for the E2F and point contacts; in the iso-constraint case their $C_i(\phi_{local})$ curves shift vertically while preserving their average slope. In the iso-volume fraction case one would expect a horizontal shift of the curves. This is however due to the statistical noise and the rather small slopes only evident in the E2F case.

The only contact type that might behave similar to sphere[47] and ellipsoid[22] in that it is described by a singular function $C_i(\phi_{local})$ independent of preparation are the F2F contacts. Figure 6 unites the six individual curves. With the possible exception of the untapped, loose sample the other curves seem indeed to be falling on one master curve.

7 Multiplicity of F2F contacts

The different nature of the F2F contacts is not only visible in their history independent $C_F 2F(\phi_{local})$. Figure 7 shows that the number of F2F contacts on any given particle are well fit by a binomial distribution (with $\chi^2 \sim 10^{-3}$); this is not the case for the E2F and point contacts.

This result implies that while the probability of forming an F2F contact grows with the proximity between particles, the formation itself is an independent random process, lacking any geometrical correlation between several neighbors. Such a behavior could be rationalized as follows: once an F2F contact is formed all three rotational degrees of freedom are completely blocked for each particle. Any additional F2F contact depends therefore solely on the capability of the incoming particle to align itself such that there is a 180 degree angle between the face normal vectors. This is however the same probability that lead already to the formation of the first F2F contact. In contrast, particles which have already established an E2F or point contact retain one or even three rotational degrees of freedom to facilitate another contact.

8 Conclusions

Because tetrahedra have four flat boundaries, their packings do not only posses point contacts similar to sphere packings but also edge-to-face and face-to-face contacts which fix larger numbers of geometrical constraints than point contacts. The number of point and edge-to-face contacts a given tetrahedron forms can neither be predicted from the global nor from the local volume fraction alone; it does depend also on the preparation history. In contrast, the formation of face-to-face contacts seems to be a stochastic process; its probability is small and increases with increasing proximity between particles. While our results support the feasibility of a mean-field approach to tetrahedra packings, they imply that the jamming paradigm in its present form will not be an adequate description.

We acknowledge computational help by Fabian Schaller.

References

[1] Farhang Radjaï and Stéphane Roux. *The Physics of Granular Media*, pages 165–187. Wiley-VCH, Weinheim, 2004.

[2] L. Vanel and E. Clément. Pressure screening and fluctuations at the bottom of a granular column. *Euro. Phys. J. B*, 11:525–533, 1999.

[3] J.F. Wambaugh, R.R. Hartley, and R.P. Behringer. Force networks and elasticity in granular silos. *Euro. Phys. J. E*, 32:135–145, 2010.

[4] Randy Back. Frictional effects on mass measurements in a column of glass beads. *Gran. Mat.*, 13:723–729, 2011.

[5] Christophe Perge, María Alejandra Aguirre, Paula Alejandra Gago, Luis A. Pugnaloni, Denis Le Tourneau, and Jean-Christophe Géminard. Evolution of pressure profiles during the discharge of a silo. *Phys. Rev. E*, 85:021303, 2012.

[6] Nikola Topić, Jason A. C. Gallas, and Thorsten Pöschel. Nonuniformities in the angle of repose and packing fraction of large heaps of particles. *Phys. Rev. Lett.*, 109:128001, 2012.

[7] Loic Vanel, Daniel Howell, D. Clark, R. P. Behringer, and Eric Clément. Memories in sand: Experimental tests of construction history on stress distributions under sandpiles. *Phys. Rev. E*, 60:R5040, 1999.

[8] Christophe Josserand, Alexei V. Tkachenko, Daniel M. Mueth, and Heinrich M. Jaeger. Memory effects in granular materials. *Phys. Rev. Lett.*, 85:3632–3635, 2000.

[9] M. Nicolas, P. Duru, and O. Pouliquen. Compaction of a granular material under cyclic shear. *Euro. Phys. J. E*, 3:309–314, 2000.

[10] A. Prados and E. Trizac. Kovacs-like memory effect in driven granular gases. *Phys. Rev. Lett.*, 112:198001, 2014.

[11] Leonardo E. Silbert, Deniz Ertaş, Gary S. Grest, Thomas C. Halsey, and Dov Levine. Geometry of frictionless and frictional sphere packings. *Phys. Rev. E*, 65:031304, 2002.

[12] H. P. Zhang and H. A. Makse. Jamming transition in emulsions and granular materials. *Phys. Rev. E*, 72:011301, 2005.

[13] Kostya Shundyak, Martin van Hecke, and Wim van Saarloos. Force mobilization and generalized isostaticity in jammed packings of frictional grains. *Phys. Rev. E*, 75:010301, 2007.

[14] S. Henkes, M. van Hecke, and W. van Saarloos. Critical jamming of frictional grains in the generalized isostaticity picture. *Europhys. Lett.*, 90:14003, 2010.

[15] Brian P. Tighe, Jacco H. Snoeijer, Thijs J. H. Vlugt, and Martin van Hecke. The force network ensemble for granular packings. *Soft Matter*, 6:2908–2917, 2010.

[16] Olivier Tsoungui, Denis Vallet, and Jean-Claude Charmet. Use of contact area trace to study the force distributions inside 2d granular systems. *Granular Matter*, 1:65–69, 1998.

[17] T. S. Majmudar and R. P. Behringer. Contact force measurements and stress-induced anisotropy in granular materials. *Nature*, 435:1079–1082, 2005.

[18] T. Aste, T. Di Matteo, M. Saadatfar, T. J. Senden, Matthias Schröter, and Harry L. Swinney. An invariant distribution in static granular media. *Europhys. Lett.*, 79:24003, 2007.

[19] G. E. Schröder-Turk, W. Mickel, M. Schröter, G. W. Delaney, M. Saadatfar, T. J. Senden, K. Mecke, and T. Aste. Disordered spherical bead packs are anisotropic. *Europhys. Lett.*, 90:34001, 2010.

[20] Andrea J. Liu and Sidney R. Nagel. The jamming transition and the marginally jammed solid. *Ann. Rev. Cond. Matt. Phys.*, 1:347–369, 2010.

[21] Martin van Hecke. Jamming of soft particles: geometry, mechanics, scaling and isostaticity. *J. Phys.: Condens. Matter*, 22:033101, 2010.

[22] Fabian M. Schaller, Max Neudecker, Mohammad Saadatfar, Gary Delaney, Gerd E. Schröder-Turk, and Matthias Schröter. Local origin of global contact numbers in frictional ellipsoid packings. *arXiv*, 1312.1327, 2015.

[23] Chaoming Song, Ping Wang, and Hernán A. Makse. A phase diagram for jammed matter. *Nature*, 453:629–632, 2008.

[24] Maxime Clusel, Eric I. Corwin, Alexander O. N. Siemens, and Jasna Brujić. A /'granocentric/' model for random packing of jammed emulsions. *Nature*, 460:611–615, 2009.

[25] Eric I. Corwin, Maxime Clusel, Alexander O. N. Siemens, and Jasna Brujić. Model for random packing of polydisperse frictionless spheres. *Soft Matter*, 6:2949–2959, 2010.

[26] James G. Puckett, Frédéric Lechenault, and Karen E. Daniels. Local origins of volume fraction fluctuations in dense granular materials. *Phys. Rev. E*, 83:041301, 2011.

[27] Ivana Agnolin and Jean-Noël Roux. Internal states of model isotropic granular packings. i. assembling process, geometry, and contact networks. *Phys. Rev. E*, 76:061302, 2007.

[28] Jie Ren, Joshua A. Dijksman, and Robert P. Behringer. Reynolds pressure and relaxation in a sheared granular system. *Physical Review Letters*, 110:018302, 2013.

[29] Dapeng Bi, Jie Zhang, Bulbul Chakraborty, and R. P. Behringer. Jamming by shear. *Nature*, 480:355–358, 2011.

[30] Max Neudecker, Stephan Ulrich, Stephan Herminghaus, and Matthias Schröter. Jammed frictional tetrahedra are hyperstatic. *Phys. Rev. Lett.*, 111:028001, 2013.

[31] Athanasios G. Athanassiadis, Marc Z. Miskin, Paul Kaplan, Nicholas Rodenberg, Seung Hwan Lee, Jason Merritt, Eric Brown, John Amend, Hod Lipson, and Heinrich M. Jaeger. Particle shape effects on the stress response of granular packings. *Soft Matter*, 10:48–59, 2013.

[32] Heinrich M. Jaeger. Celebrating soft matters 10th anniversary: Toward jamming by design. *Soft Matter*, 11:12–27, 2015.

[33] Jessica Baker and Arshad Kudrolli. Maximum and minimum stable random packings of platonic solids. *Phys. Rev. E*, 82:061304, 2010.

[34] Amir Haji-Akbari, Michael Engel, Aaron S. Keys, Xiaoyu Zheng, Rolfe G. Petschek, Peter Palffy-Muhoray, and Sharon C. Glotzer. Disordered, quasicrystalline and crystalline phases of densely packed tetrahedra. *Nature*, 462:773–777, 2009.

[35] S. Torquato and Y. Jiao. Dense packings of the platonic and archimedean solids. *Nature*, 460:876–879, 2009.

[36] Kyle C. Smith, Meheboob Alam, and Timothy S. Fisher. Athermal jamming of soft frictionless platonic solids. *Phys. Rev. E*, 82:051304, 2010.

[37] Kyle C. Smith, Timothy S. Fisher, and Meheboob Alam. Isostaticity of constraints in amorphous jammed systems of soft frictionless platonic solids. *Phys. Rev. E*, 84:030301, 2011.

[38] Yang Jiao and Salvatore Torquato. Maximally random jammed packings of platonic solids: Hyperuniform long-range correlations and isostaticity. *Phys. Rev. E*, 84:041309, 2011.

[39] Shuixiang Li, Peng Lu, Weiwei Jin, and Lingyi Meng. Quasi-random packing of tetrahedra. *Soft Matter*, 9:9298–9302, 2013.

[40] Kyle C. Smith, Ishan Srivastava, Timothy S. Fisher, and Meheboob Alam. Variable-cell method for stress-controlled jamming of athermal, frictionless grains. *Phys. Rev. E*, 89:042203, 2014.

[41] Lufeng Liu, Peng Lu, Lingyi Meng, Weiwei Jin, and Shuixiang Li. Excluded volumes of clusters in tetrahedral particle packing. *Physics Letters A*, 378:835–838, 2014.

[42] Adrian Baule, Romain Mari, Lin Bo, Louis Portal, and Hernn A. Makse. Mean-field theory of random close packings of axisymmetric particles. *Nat Commun*, 4:1–11, 2013.

[43] Adrian Baule and Hernán A. Makse. Fundamental challenges in packing problems: from spherical to non-spherical particles. *Soft Matter*, 10:4423–4429, 2014.

[44] Alexander Jaoshvili, Andria Esakia, Massimo Porrati, and Paul M. Chaikin. Experiments on the random packing of tetrahedral dice. *Phys. Rev. Lett.*, 104:185501, 2010.

[45] μ_s is computed from the tangens of the inclination angle where a face to face contact starts to slide.

[46] DOI from Dryad; data upload is only possible after paper is accepted by a journal.

[47] T Aste, M Saadatfar, and T J Senden. Local and global relations between the number of contacts and density in monodisperse sphere packs. *J. Stat. Mech.: Theory and Exp.*, 2006:P07010, 2006.

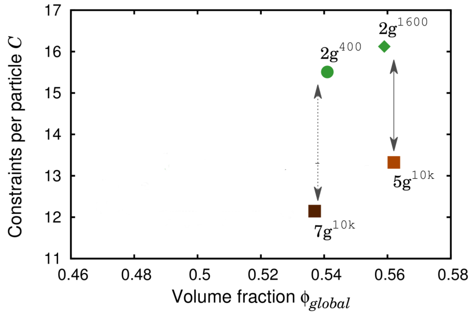

experiment	ϕ	C	C_{F2F}	C_{E2F}	C_{point}
$2g^{400}$	0.541	15.5	0.63	6.3	8.6
$7g^{10k}$	0.537	12.1	0.73	4.9	6.5
$2g^{1600}$	0.559	16.1	1.07	6.6	8.4
$5g^{10k}$	0.562	13.3	0.96	5.4	6.9

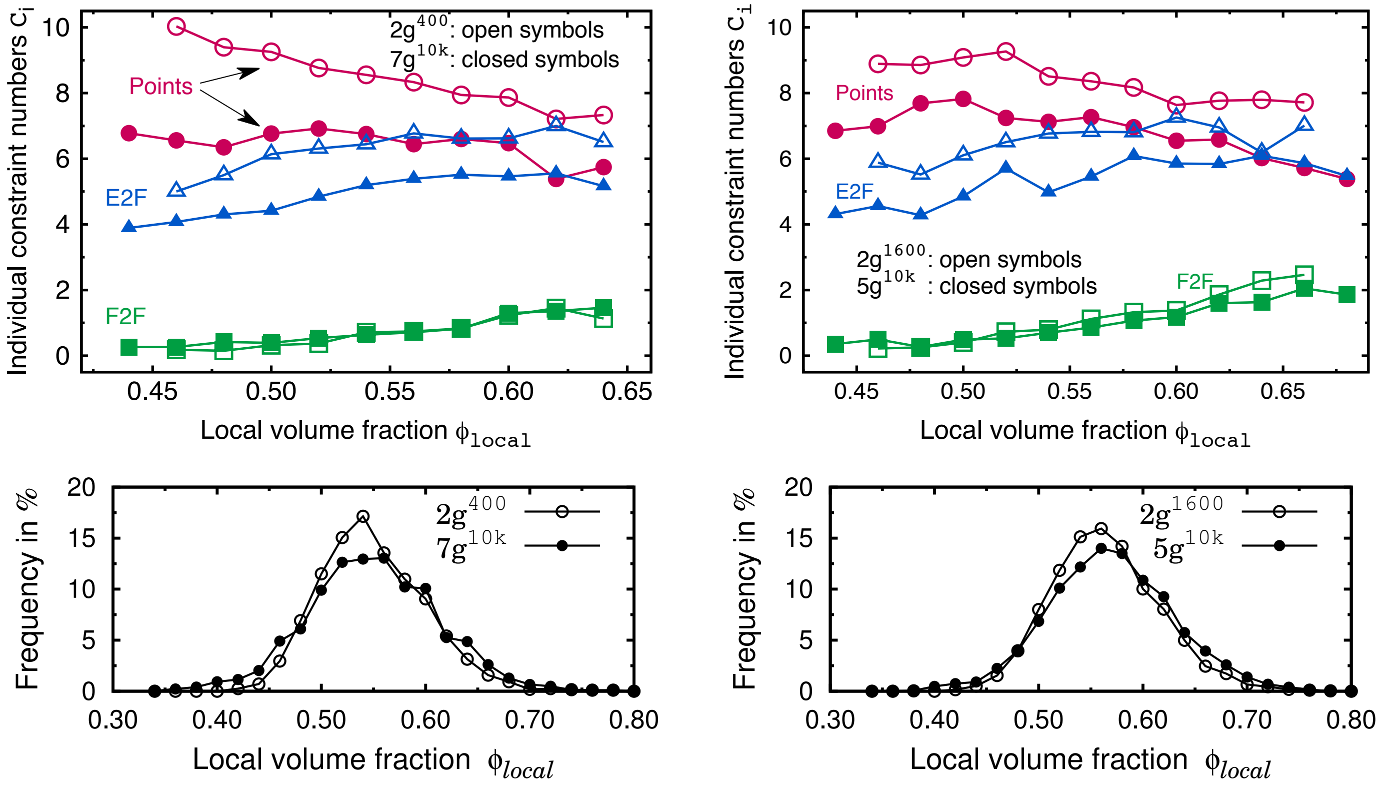

Figure 4 Iso-volume fraction pairs. In all panels the open symbols correspond to the experiment with the higher C. The local analysis in the middle row of panels shows how the contribution of the different constraint types depends on the local volume fraction. Nearly the total increase in C for the $2g^{400}$ and $2g^{1600}$ packings is contributed by the E2F and point contacts. At the same time the slope $dC/d\phi_{local}$ stays constant. C_i values are computed for all bins with more than 1.7 % of the totally analyzed particles. The bottom row of panels show the probability distribution of ϕ_{local} which suggest little influence of preparation.

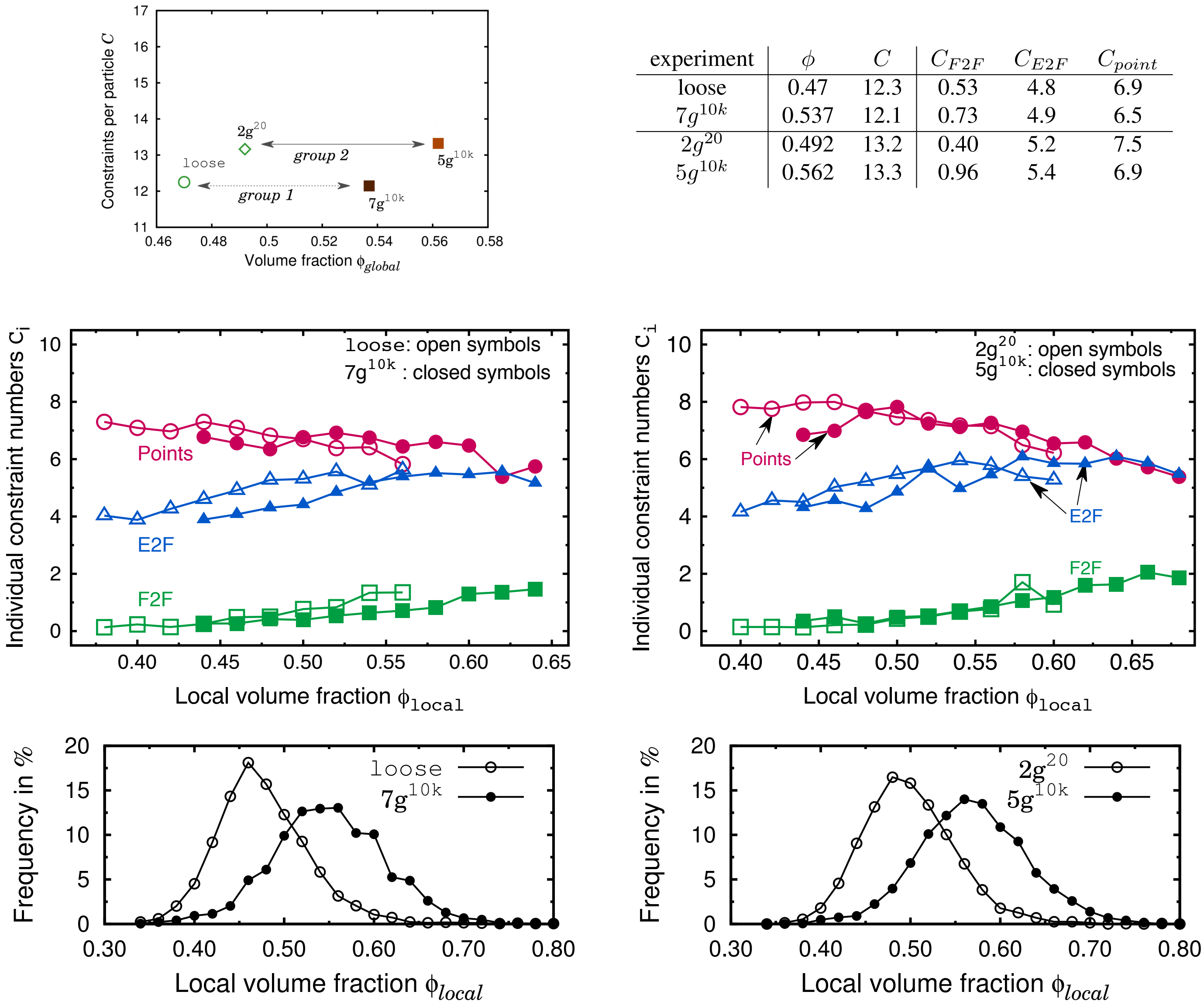

experiment	ϕ	C	C_{F2F}	C_{E2F}	C_{point}
loose	0.47	12.3	0.53	4.8	6.9
$7g^{10k}$	0.537	12.1	0.73	4.9	6.5
$2g^{20}$	0.492	13.2	0.40	5.2	7.5
$5g^{10k}$	0.562	13.3	0.96	5.4	6.9

Figure 5 Iso-constraint pairs. In all panels the open symbols correspond to the experiment with the lower ϕ_{global}. The local analysis in the middle row of panels shows how the contribution of the different constraint types depends on the local volume fraction. While C_{E2F} versus ϕ_{local} display a horizontal shift with increasing ϕ_{global}, systematic changes for the point and F2F contacts are more difficult to deduce. C_i values are computed for all bins with more than 1.7 % of the total number of analyzed particles. The bottom row of panels show the probability distribution of ϕ_{local} which broadens with increasing ϕ_{global}.

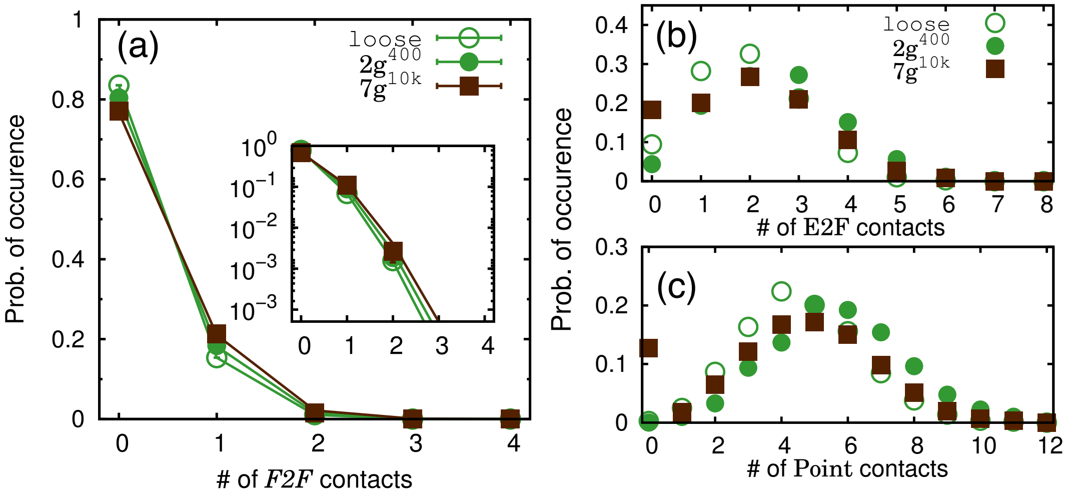

Figure 7 Probability of particles having multiple contacts of the same type. (a) Frequency distribution of the number of face-to-face contacts. Straight lines are fits with a binomial distribution resulting in p values of 0.044 (loose), 0.054 ($2g^{400}$), and 0.064 ($7g^{10k}$). In contrast, the multiplicity of the E2F (panel b) and point contacts (panel c) is not described by a binomial distribution.